Appl Magn Reson (2012) 42:393–402
DOI 10.1007/s00723-011-0306-5

Applied
Magnetic Resonance

A Simple Model for Understanding the Origin of the Amide Proton Transfer MRI Signal in Tissue

Jinyuan Zhou · Kun Yan · He Zhu

Received: 29 October 2011 / Published online: 10 January 2012

Abstract Amide proton transfer (APT) imaging is a new molecular magnetic resonance imaging (MRI) technique that gives contrast at the cellular protein level. To better understand the origin of the APT signal in tissue, fresh and cooked hen eggs ($n = 4$) were imaged at 4.7 T. The APT effect was quantified using the asymmetry in the magnetization transfer ratio (MTR_{asym}) at the composite amide proton resonance frequency (3.5 ppm from the water resonance). The measured APT signals were significantly higher in the fresh egg white ($20.1 \pm 0.9\%$) than in the fresh egg yolk ($-1.4 \pm 1.1\%$; $P < 0.001$), and in the cooked egg white ($2.8 \pm 0.7\%$; $P < 0.001$), all of which have similar absolute protein contents. The data support the notion that the APT effect observed in vivo is associated with mobile proteins in tissue, such as those in the cytoplasm.

1 Introduction

Chemical exchange-dependent saturation transfer (CEST) imaging is a novel molecular magnetic resonance imaging (MRI) technique that allows indirect detection of low-concentration, endogenous or exogenous solute molecules via the bulk water signal [1–3]. Using small molecules in solution, Balaban et al. [1] first demonstrated that the process of saturation transfer between exchangeable solute protons and water protons could be used to enhance the sensitivity of metabolite

J. Zhou (✉) · K. Yan · H. Zhu
Neurosection, Division of MR Research, Department of Radiology,
Johns Hopkins University School of Medicine, 600 N. Wolfe Street,
336 Park Building, Baltimore, MD 21287, USA
e-mail: jzhou@mri.jhu.edu

J. Zhou · H. Zhu
F.M. Kirby Research Center for Functional Brain Imaging, Kennedy Krieger Institute,
Baltimore, MD 21205, USA

imaging. After this pioneering work, van Zijl et al. [4] showed that an enormous increase in detection sensitivity could be obtained for macromolecules, such as poly-L-lysine and dendrimers, with a large number of exchange sites of similar chemical shifts. Sherry et al. [5] and Aime et al. [6] reported several paramagnetic CEST agents (lanthanide complexes; usually called paraCEST) that made the approach more flexible, by significantly enlarging the frequency range for the exchange sites. Unique from the relaxation-based MRI contrast mechanism commonly used in the clinic, such as T_2 and T_1, this exchange-based approach presents not only a large sensitivity enhancement, through saturation accumulation on the water signal, but also a specific image contrast that can be switched on and off at will, by turning on and off the radiofrequency (RF) irradiation or by changing the irradiation frequency.

The CEST-based MRI technology allows multiple new types of applications; however, more work is required to realize the potential of this technology in the clinical setting. Currently, one of the successful human applications is the amide proton transfer (APT) approach [7], in which the composite backbone amide resonance of endogenous mobile proteins [8], around 8.3 ppm in the in vivo proton NMR spectrum, is labeled using selective RF saturation and detected indirectly through the bulk water signal to image pH [7, 9, 10], or the protein content of tissue, especially in tumor [11–15], where many proteins are over-expressed. APT imaging is able to extend MRI contrast to the endogenous protein level. In principle, if proteins are in a more liquid compartment (such as in the cytoplasm) within a cell, they could be potentially detected by APT. However, the cellular origin of this APT image contrast in biological tissues is not yet completely clear. Interestingly, a fresh hen egg happens to present a big cytoplasmic compartment (egg white) that contains a high-protein concentration. In addition, the fresh and cooked egg whites have often been used as a phantom to analyze the changes in MRI properties of biological tissues [16, 17]. In this paper, by comparing the APT effects in a fresh egg white with those in a fresh egg yolk and a cooked egg white, we further postulate that the APT signals measured in vivo do, indeed, originate predominantly from endogenous mobile proteins, such as those in the cytoplasm.

2 Materials and Methods

2.1 Phantoms

Fresh hen eggs were acquired commercially. After the first MRI measurement was performed, these eggs were cooked in 100°C water for 10 min and cooled to room temperature. The second MRI measurement was obtained 2–3 h after cooking.

2.2 MRI Experiments

MRI data were acquired using a horizontal bore 4.7 T Biospec animal imager with a volume coil with the internal diameter (ID) of 8 cm for RF transmission and reception. We used a weak continuous-wave, off-resonance RF irradiation (duration, 4 s; power level, 2 μT) for the APT imaging. Single-shot, spin-echo

echo-planar imaging was used for the data acquisition. The image matrix was 64 × 64; the field of view was 32 × 32 mm^2; the slice thickness was 2 mm; the repetition time (TR) was 10 s; and the echo time (TE) was 30 ms. The magnetization transfer (MT) spectrum was acquired over an offset range of ±6 ppm with an interval of 0.5 ppm (S_{sat}). One image was acquired per offset. A corresponding control image in the absence of RF saturation (S_0) was acquired for imaging signal intensity normalization.

In addition, T_2 mapping (TR, 3 s; TE, 30, 40, 50, 60, 70, 80, and 90 ms; number of averages, 4) and T_1 mapping using the inversion recovery sequence (predelay, 3 s; TE, 30 ms; inversion recovery time, 0.05, 0.3, 0.6, 1.2, 1.8, 2.5, and 3.5 s; number of averages, 4) were also performed.

2.3 Data Analysis

Data processing was performed using the IDL software (Research Systems, Inc., Boulder, CO, USA). The measured MT spectra (S_{sat}/S_0 plotted as a function of saturation frequency offset, relative to water, which was assigned to be at 0 ppm) were corrected for field inhomogeneity effects on a pixel-by-pixel basis according to the procedure used in vivo [12]. To quantify the APT effect, as described previously [7], we used the magnetization-transfer-ratio (MTR = $1-S_{sat}/S_0$) asymmetry parameter, MTR_{asym}, by subtracting the MTR values, obtained at the negative offset with respect to water, from those at the corresponding positive offset:

$$\begin{aligned} MTR_{asym}(\text{offset}) &= MTR(+\text{offset}) - MTR(-\text{offset}) \\ &= S_{sat}(-\text{offset})/S_0 - S_{sat}(+\text{offset})/S_0. \end{aligned} \tag{1}$$

Particularly, the APT effects were quantified according to the equation:

$$MTR_{asym}(3.5\,\text{ppm}) = S_{sat}(-3.5\,\text{ppm})/S_0 - S_{sat}(3.5\,\text{ppm})/S_0. \tag{2}$$

The spin–spin relaxation time of water, T_2, was fitted using the equation: $I = A\ \exp(-\text{TE}/T_2)$. The spin–lattice relaxation time of water, T_1, was fitted with a three-parameter (B, C, T_1) equation: $I = B + C\exp(-\text{TI}/T_1)$, where B was used to calculate the relative water content for egg yolk with respect to egg white.

3 Results

Figure 1a–c shows the experimental results of APT imaging on the fresh egg white and the fresh egg yolk ($n = 4$). Similar to the in vivo case [12], the RF irradiation reduced the signal intensities over the complete spectral range on the MT spectrum (Fig. 1a). This is mainly due to the direct water saturation effect, close to the water frequency, and the magnetization transfer contrast (MTC) effect, over the whole spectral range, associated with immobile macromolecules in tissue [18]. There was an extra signal reduction at a frequency offset of about 3–3.5 ppm from water in the fresh egg-white MT spectrum. Using 4.75 ppm for the water resonance, this corresponds to the spectral frequency of the combined amide proton resonance

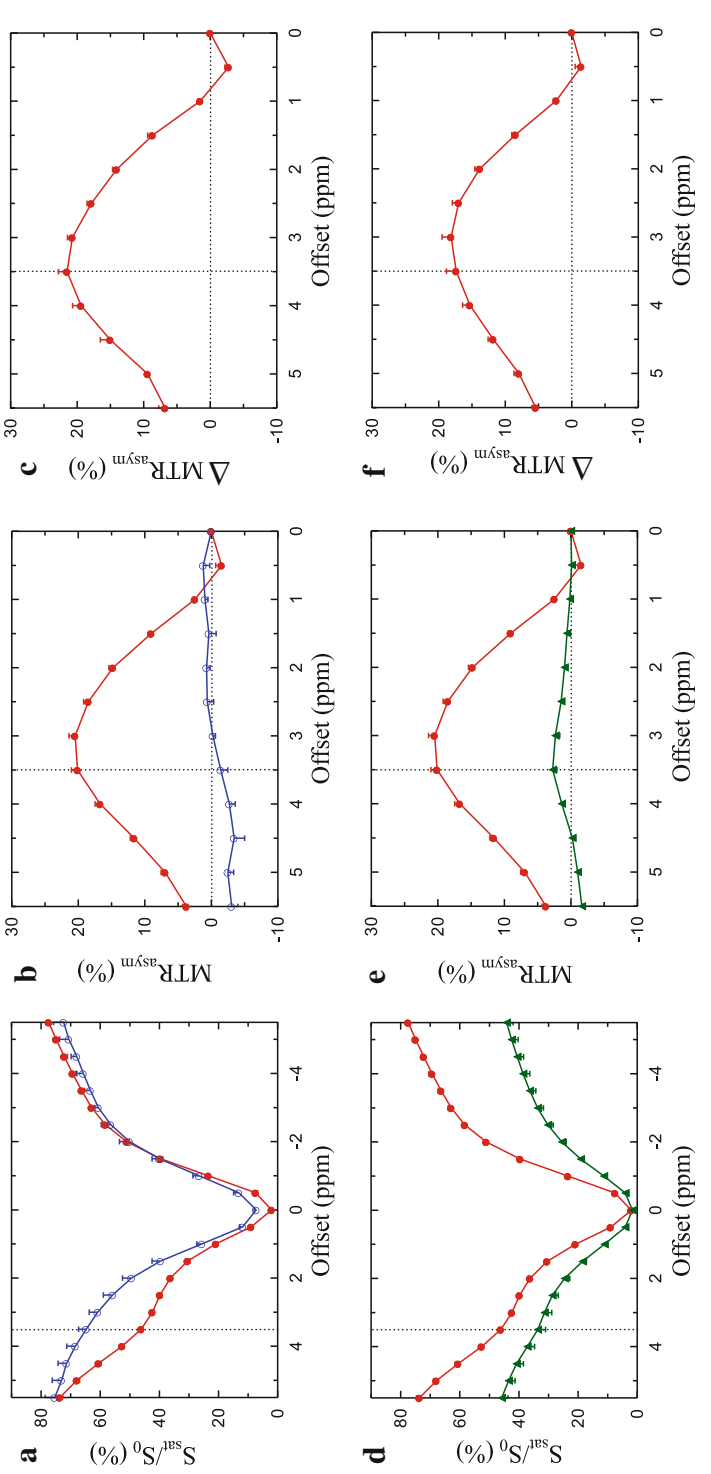

Fig. 1 **a–c** MT, MTR_{asym}, and ΔMTR_{asym} spectra measured for the fresh egg white (*solid circles*) and egg yolk (*open circles*, $n = 4$). The large dip at the frequency offset of 3.5 ppm (corresponding to the amide resonance frequency) in the fresh egg white MT spectrum (**a**) clearly indicates the existence of the APT effect, which gives rise to a large positive MT difference in the resulting asymmetry curve (**b**). In contrast, the effect of APT is negligible in the fresh egg yolk. The MTR_{asym} change between the fresh egg white and yolk (**c**) is maximized at offset 3.5 ppm. **d–f** MT, MTR_{asym}, and ΔMTR_{asym} spectra measured for the fresh (*solid circles*) and cooked egg white (*triangles*, $n = 4$). The effect of MTC is increased in the cooked egg white (**d**), but the effect of APT is largely reduced (**e**), because all proteins were denatured and became opaque

around 8.3 ppm, indicating that this large extra signal reduction originates predominantly from the amide protons of the mobile proteins. This interesting APT imaging feature, seen in the fresh egg-white MT curve, did not exist in the fresh egg-yolk MT curve, indicating a very small to negligible APT effect in the fresh egg yolk.

The presence of the APT effect became more obvious when MTR asymmetry analysis was used to remove the influence of the direct saturation and MTC (Fig. 1b). However, this MTR_{asym}(3.5 ppm) effect cannot be assigned solely to APT, because the solid-like MTC effect is somewhat asymmetric with respect to the water resonance, with a center frequency in the aliphatic range [19]. The fact that the MTR_{asym} plot for the fresh egg white was not maximized at the offset of 3.5 ppm can be attributed to the negative MTC asymmetry background. This can be clearly seen in the MTR_{asym} plot for the fresh egg yolk, in which the APT effect was likely negligible and the measured MTR_{asym}(3.5 ppm) value negative at the offsets of >3 ppm. However, when comparing the fresh egg-white MTR_{asym} plot with the fresh egg-yolk MTR_{asym} plot (Fig. 1c), the maximum change in MTR_{asym} appeared at an offset of 3.5 ppm from water, indicating that this difference, indeed, originates from the amide protons of the mobile proteins.

Figure 1d–f compares the results of APT imaging on fresh and cooked egg whites ($n = 4$). The measured MT spectrum of the cooked egg white became much broader than that of the fresh egg white (Fig. 1d), as reported in a previous study [17]. This occurred because both the direct water saturation and solid-like MTC effects were strongly increased after the egg was cooked and the proteins denatured. The resulting MTR_{asym} plot for the cooked egg white (Fig. 1e) shows a varying MTR asymmetry that was initially positive and then negative at the offsets of >4.5 ppm, a characteristic similar to brain tissue in vivo when using APT imaging [7]. Again, this is due to the fact that the solid-like MTC effect is, to some extent, asymmetric with respect to the water resonance [19]. Interestingly, the APT effect was greatly reduced after the egg was cooked; however, proteomics experiments showed that the protein profiles were roughly similar in the fresh and cooked egg whites (see "Appendix").

Figure 2 shows two examples of the APT images of the fresh and cooked eggs. The APT effects were significantly higher in the fresh egg white than in the fresh egg yolk, as well as in the cooked egg white and yolk. A larger APT image contrast can be seen between the fresh egg white and yolk.

Table 1 summarizes the measured water T_1, T_2, water content, and MTR_{asym} (3.5 ppm) of the fresh egg white, fresh egg yolk, and cooked egg white. These results for T_1 and T_2 values agrees well with a previous report at the same field strength (4.7 T) [16]. The shorter T_1 and T_2 values in the fresh egg yolk tentatively attributed to its large lipid content. The measured MTR_{asym}(3.5 ppm) values were 20.1 ± 0.9% in the fresh egg white and −1.4 ± 1.1% in the fresh egg yolk, and the difference was highly significant ($P < 0.001$). The MTR_{asym}(3.5 ppm) value in the cooked egg white was as low as 2.8 ± 0.7%, significantly smaller than that measured in the fresh egg white (20.1 ± 0.9%; $P < 0.001$). Note that the APT effects were not reported in the previous studies [17], where much higher RF saturation power levels were used and the water intensities at the offset of 3.5 ppm were almost zero.

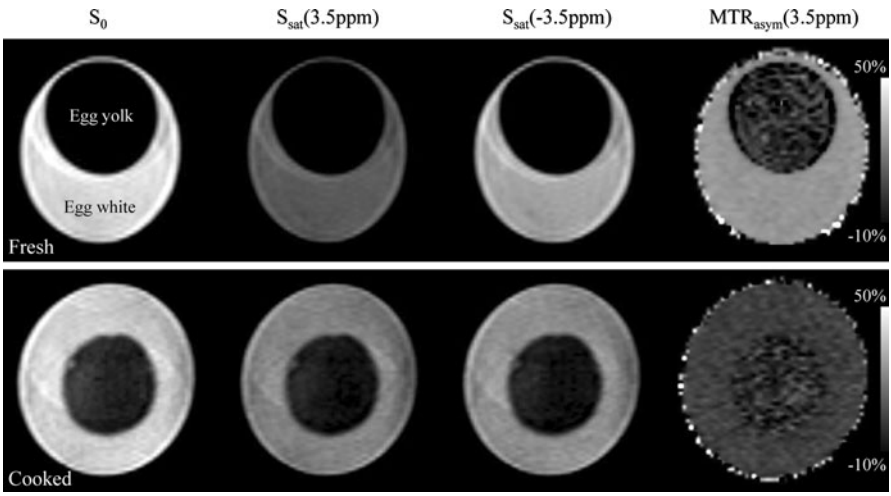

Fig. 2 Examples of the APT images of the fresh (*top row*) and cooked (*bottom row*) hen eggs. The APT signals, defined as MTR_{asym}(3.5 ppm), were quantified according to Eq. (2)

Table 1 MRI parameters measured for the fresh and cooked eggs ($n = 4$)

Sample	Water T_2 (ms)	Water T_1 (s)	Relative water content	MTR_{asym}(3.5 ppm) (% water intensity)
Fresh egg white	166.8 ± 10.5	1.88 ± 0.04	1	20.1 ± 0.9
Fresh egg yolk	38.0 ± 2.0$^+$	0.26 ± 0.03$^+$	0.22 ± 0.05$^+$	−1.4 ± 1.1$^+$
Cooked egg white	61.8 ± 8.9$^+$	1.83 ± 0.09	No data	2.8 ± 0.7$^+$

$^+$ The differences between the fresh egg white and yolk or between the fresh egg white and cooked egg white were significant (all $P < 0.001$)

4 Discussion

As discussed in our previous paper [7], the measured APT-MRI signal intensities in tissue can approximately be described as:

$$\mathrm{MTR_{asym}}(3.5\,\mathrm{ppm}) = \mathrm{MTR'_{asym}}(3.5\,\mathrm{ppm}) + \mathrm{APTR}, \quad (3)$$

where MTR'_{asym}(3.5 ppm) may include the inherent asymmetry of the solid-phase macromolecular MTC effect [19], and the intramolecular and intermolecular nuclear Overhauser effects (NOE) of aliphatic protons of mobile macromolecules and metabolites [20], and APTR is the proton transfer ratio for the amide protons of mobile cellular proteins. Because MTR'_{asym}(3.5 ppm) has a complicated origin and is unknown, it is difficult to quantify the actual APTR value in tissue. However, because MTR'_{asym}(3.5 ppm) is negative, the APTR values can be concluded to be larger than 20.1 ± 0.9% in the fresh egg white and larger than 2.8 ± 0.7% in the cooked egg white. In the fresh egg yolk, the APTR values were seemingly small;

therefore, the measured $MTR_{asym}(3.5\ ppm)$ values were apparently negative [mainly dominated by the term $MTR'_{asym}(3.5\ ppm)$].

On the basis of a two-pool proton exchange model (small solute pool, large water pool), APTR can be written as [7]:

$$APTR = k_{sw} \cdot ([\text{amide proton}]/[\text{water proton}]) \cdot T_1 \cdot \left(1 - e^{-t_{sat}/T_1}\right), \quad (4)$$

where k_{sw} is the average solute-to-water proton exchange rate over all amide protons participating in the effect, square brackets indicate the concentration, T_1 is the longitudinal relaxation time of water, and t_{sat} is the RF saturation time, which is also the effective time during which APT occurs. The water proton concentration is $2 \times 55\ M \times$ tissue water content in an MRI voxel. In our case, $1-\exp(-t_{sat}/T_1) \approx 1$. The egg white is the cytoplasm of the egg, which is a gelatinous, semi-transparent liquid mixture with about 11% proteins [21]. The egg yolk is the nucleus of the egg. The yolk is relatively solid and contains proteins ($\sim$16%), fat, cholesterol, carbohydrates, etc. [21]. Our experimental results clearly show that the effects of APT were much larger in the fresh egg white than in the fresh egg yolk (20.1 vs. -1.4%). According to Eq. [4] and the ratios of the measured water T_1 and water content (Table 1), this negligible APT effect in the fresh egg yolk (short water T_1 and low water content, ratio 1.18), with respect to the fresh egg white (long water T_1 and high-water content, ratio 1.88), may dominantly reflect the smaller mobile amide concentration in the fresh egg yolk (assume a similar k_{sw} in these two compartments).

After the egg was cooked, many proteins were denatured. The heat-induced aggregation and conformational changes of egg white proteins were investigated in more detail previously [22, 23]. Our extra experiments showed that the protein profiles of the fresh and cooked egg whites were roughly similar (see "Appendix"). The heat-denatured egg white became solid-like, as demonstrated by the increased MTC effect (Fig. 1d). Upon the thermal denaturation, the decreased mobility would significantly broaden the amide resonance signal, leading to the loss of the specific APT effect at the offset of 3.5 ppm. In this study, the APT signals were greatly reduced (from 20.1% in the fresh egg white to 2.8% in the cooked egg white). The decreased mobility of proteins in the cooked egg white could be a main factor for this APT reduction, although the increased MTC may competitively decrease the APT effect.

The cytoplasm makes up about 70% of the cell volume and is composed of water, proteins, and other chemicals. The experimental results obtained from the fresh and cooked eggs support our hypothesis that the in vivo APT signals are associated with mobile cellular proteins [7], such as those dissolved in the liquid-like cytosol. When proteins are in such a liquid-like compartment, they have a narrow resonance signal. Although these molecules generally occur at low concentrations in tissue, they each contain multiple backbone amide groups. Moreover, these backbone amide groups resonate at about the same nuclear magnetic resonance (NMR) frequency, namely 8.1–8.8 ppm [8], leading to a large composite amide proton resonance at the offset of $\sim$3.5 ppm from water [7]. Thus, these mobile proteins could be potentially detected as a whole by APT MRI. On the other hand, when proteins stay in a more

solid environment of the cell, such as in the nucleus and the membrane, they could generally not be measured by APT imaging.

Finally, it is important to mention that there are generally multiple types of exchangeable protons and, thus, multiple CEST effects in biological tissues. For example, most protein side chain exchangeable protons resonate at 6.6–7.6 ppm in the proton NMR spectrum [8], which may generate a detectable CEST effect at ~2 ppm from water [11, 12]. However, the fact that the maximum change between the fresh egg-white and egg-yolk MTR_{asym} plots appeared at an offset of 3.5 ppm from water reflects that this difference dominantly originates from the amide protons of the mobile proteins.

5 Conclusions

We have demonstrated that the APT imaging intensities are significantly higher in fresh liquid-like egg white than in fresh solid-like egg yolk, and in cooked solid-like egg white. The fact that these samples have similar protein content, but very different APT effects, clearly shows that the presence of the APT effect depends on the mobility of cellular proteins and peptides. The APT effect measured in tissue must come from the contributions of mobile proteins and peptides, such as those dissolved in the cytosol.

Acknowledgments We thank Dr. Peter van Zijl for helpful comments and Ms. Mary McAllister for editorial assistance. This work was supported in part by grants from NIH (EB009112, EB009731), and the Dana Foundation.

Appendix

Proteomic Analyses of the Fresh and Cooked Egg Whites

Protein extraction was performed using the PlusOne Sample Grinding Kit (GE Healthcare) according to the manufacture's recommended protocol. Fresh and cooked egg white (~200 mg) were lysed with 1 mL lysis buffer (8 M urea, 2 M thiourea, 4% CHAPS, 1% DTT) separately. After centrifuging for 10 min at a maximum speed, clear supernatant was collected carefully. Protein labeling was performed for fluorescence two-dimensional (2-D) differential in-gel expression (DIGE) technology (GE Healthcare) according to the manufacturer's recommended protocol. Each protein sample (50 μl) was labeled with a different fluorophore. The labeling mixture was subjected to 2D gel electrophoresis following protocols for pH 4–7. CyDye-labeled proteins were visualized using a Typhoon 9410 imager (GE Healthcare) and the images were shown in the black-white.

As reported previously [24, 25], several high-concentration proteins, such as ovalbumin, ovalbumin X, ovalbumin Y, ovotransferrin, ovoglycoprotein, ovoinhibitor, TENP, clusterin, and Hep21 protein, can be clearly observed in both fresh and cooked egg whites (Fig. 3). Of these, ovalbumin (45 kDa) is the most abundant

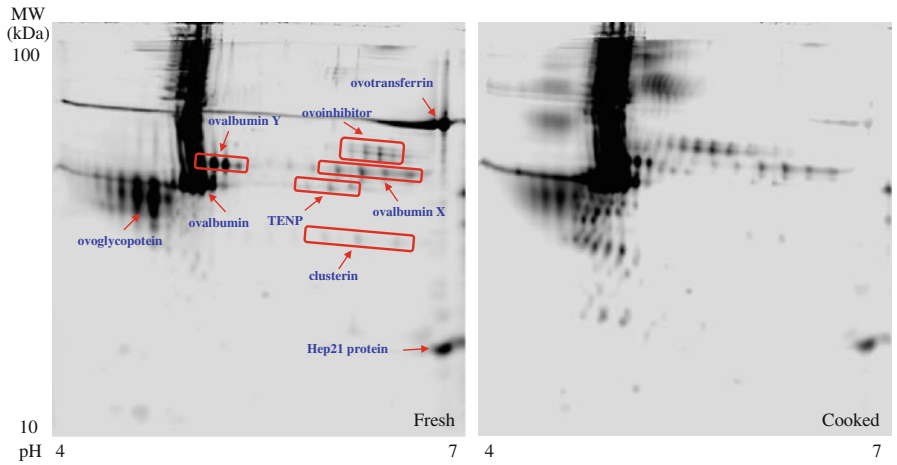

Fig. 3 2D-DIGE images of the egg-white proteins from the fresh (*left*) and cooked (*right*) hen eggs. *Nine large spots* (ovalbumin, ovalbumin X, ovalbumin Y, ovotransferrin, ovoglycoprotein, ovoinhibitor, TENP, clusterin, Hep21 protein) are clearly visual in both gel images. The contents of most of these proteins were comparable in the two images, except two heat-sensitive proteins (ovotransferrin, ovoglycoprotein), whose concentrations reduced in the cooked case

protein that constitutes 54% of the total egg white proteins. Most proteins, including ovalbumin, didn't show large changes after the thermal denaturation. However, the concentrations of ovotransferrin and ovoglycoprotein were decreased due to their heat-sensitive properties.

References

1. K.M. Ward, A.H. Aletras, R.S. Balaban, J. Magn. Reson. **143**, 79–87 (2000)
2. J. Zhou, P.C. van Zijl, Progr. NMR Spectr. **48**, 109–136 (2006)
3. I. Hancu, W.T. Dixon, M. Woods, E. Vinogradov, A.D. Sherry, R.E. Lenkinski, Acta Radiol. **51**, 910–923 (2010)
4. N. Goffeney, J.W.M. Bulte, J. Duyn, L.H. Bryant, P.C.M. van Zijl, J. Am. Chem. Soc. **123**, 8628–8629 (2001)
5. S. Zhang, P. Winter, K. Wu, A.D. Sherry, J. Am. Chem. Soc. **123**(7), 1517–1578 (2001)
6. S. Aime, A. Barge, D. Delli Castelli, F. Fedeli, A. Mortillaro, F.U. Nielsen, E. Terreno, Magn. Reson. Med. **47**, 639–648 (2002)
7. J. Zhou, J. Payen, D.A. Wilson, R.J. Traystman, P.C.M. van Zijl, Nature Med. **9**, 1085–1090 (2003)
8. K. Wuthrich, *NMR of proteins and nucleic acids* (John Wiley & Sons, New York, 1986)
9. P.Z. Sun, J. Zhou, W. Sun, J. Huang, P.C.M. van Zijl, J. Cereb. Blood Flow Metab. **27**, 1129–1136 (2007)
10. K.T. Jokivarsi, H.I. Grohn, O.H. Grohn, R.A. Kauppinen, Magn. Reson. Med. **57**, 647–653 (2007)
11. J. Zhou, B. Lal, D.A. Wilson, J. Laterra, P.C.M. van Zijl, Magn. Reson. Med. **50**, 1120–1126 (2003)
12. A. Salhotra, B. Lal, J. Laterra, P.Z. Sun, P.C.M. van Zijl, J. Zhou, NMR Biomed. **21**, 489–497 (2008)
13. J. Zhou, J.O. Blakeley, J. Hua, M. Kim, J. Laterra, M.G. Pomper, P.C.M. van Zijl, Magn. Reson. Med. **60**, 842–849 (2008)
14. Z. Wen, S. Hu, F. Huang, X. Wang, L. Guo, X. Quan, S. Wang, J. Zhou, NeuroImage **51**, 616–622 (2010)
15. J. Zhou, E. Tryggestad, Z. Wen, B. Lal, T. Zhou, R. Grossman, S. Wang, K. Yan, D.-X. Fu, E. Ford, B. Tyler, J. Blakeley, J. Laterra, P.C.M. van Zijl, Nature Med. **17**, 130–134 (2011)

16. R. Jayasundar, S. Ayyar, P. Raghunathan, Magn. Reson. Imag. **15**, 709–717 (1997)
17. S.J. Graham, G.J. Stanisz, A. Kecojevic, M.J. Bronskill, R.M. Henkelman, Magn. Reson. Med. **42**, 1061–1071 (1999)
18. R.M. Henkelman, G.J. Stanisz, S.J. Graham, NMR Biomed. **14**, 57–64 (2001)
19. J. Hua, C.K. Jones, J. Blakeley, S.A. Smith, P.C.M. van Zijl, J. Zhou, Magn. Reson. Med. **58**, 786–793 (2007)
20. W. Ling, R.R. Regatte, G. Navon, A. Jerschow, Proc. Natl. Acad. Sci. USA **105**, 2266–2270 (2008)
21. T. Kaewmanee, S. Benjakul, W. Visessanguan, Food Chem. **112**, 560–569 (2009)
22. M.B. Smith, J.F. Back, Nature **193**, 878–879 (1962)
23. Y. Mine, T. Noutomi, N. Haga, J. Agric. Food Chem. **38**, 2122–2125 (1990)
24. C. Guerin-Dubiard, M. Pasco, D. Molle, C. Desert, T. Croguennec, F. Nau, J. Agric. Food Chem. **54**, 3901–3910 (2006)
25. D.A. Omana, Y. Liang, N.N.V. Kav, J. Wu, Proteomics **11**, 144–153 (2011)